Journal of the Palaeontological Society of India
Volume 67(1), June 30, 2022: 211-219

ISSN 0552-9360

Some aspects of depositional and petrographic frameworks of carbonate rocks of the late Neoproterozoic Krol Group, Lesser Himalaya, India

Aninda Mazumdar

JPSI

Late Neoproterozoic carbonate deposits are well documented from the Krol Belt, Lesser Himalaya. The Krol A and Krol B Formations of the Krol Group are characterized primarily by a succession of micritic limestone/ marl and red/green shales, respectively. In contrast, the Krol C and D Formations are characterized by thick sequences of limestone and dolomite showing deep subtidal to supratidal/ karstic depositional features. Petrographic textures recorded in Krol C and D carbonate rocks include fenestral void filling/ fascicular optic type fibrous dolomites; dedolomitisation features, cloudy center clear rim dolomite (CCCR texture), Baroque dolomite, chert-dolomite association, oolites, cementation of algal mat fragments and anastomosing microstylolitic (non-sutured) seam solution. Both early and burial diagenetic textures are observed in these carbonate rocks. The petrographic studies may help to understand the diagenetic evolution Krol carbonates, including early and burial dolomitization pathways.

ARTICLE HISTORY

Manuscript received: 28/04/2022
Manuscript accepted: 26/05/2022

Keywords: Neoproterozoic-Krol-Carbonate, Deposition Petrography

Geological Oceanography, CSIR-National Institute of Oceanography, Dona Paula, Goa-403004, India. Corresponding author's e-mail: maninda@nio.org

INTRODUCTION

Extensive carbonates and evaporites deposits have been reported from the late Neoproterozoic (Ediacaran Period, ca. 635–541 Ma) sedimentary sequences of India (Jiang *et al.,* 2002; Jiang *et al.,* 2003a,b,c; Jain *et al.,* 2020), South China (Jiang *et al.,* 2003c and 2006), North China (Xiao *et al.,* 2014), Oman (Becker *et al.,* 2019), Australia (Schmid, 2017) and Pakistan (Hussain, 2021). Sequence stratigraphy combined with chemostratigraphic analyses of these sedimentary deposits helped to understand early animal evolutions and global chemo-stratigraphic correlation (Mazumdar and Banerjee, 1998; Kaufman *et al.,* 2006; Mazumdar and Strauss, 2006; Xiao *et al.,* 2022). Geological, geochemical and palaeontological studies have contributed to palaeogeographic reconstruction in southern China, India and Australia during the late Neoproterozoic-Cambrian period (Jiang *et al.,* 2003c). The reconstruction suggests eustatic influence on stratigraphic development as well as paleogeographic affinity. The late Neoproterozoic shallow marine carbonate and clastic rocks of lesser Himalaya, India, have been extensively studied for sedimentological and geochemical aspects by many workers over the last few decades (Singh *et al.,* 1980; Singh and Rai, 1983; Aharon *et al.,* 1987; Mazumdar, 1996; Jiang *et al.,* 2002; Jiang *et al.,* 2003b; Jiang *et al.,* 2006, and Kaufman *et al.,* 2006). The studies have revealed a late Neoproterozoic glaciation phase, followed by extensive deposition of siliciclastic sediments and massive sequences of limestone and dolomites (Krol Group). The early Cambrian Tal Group overlies the carbonate rocks of the Krol Group.

The sedimentary structures in the calcareous sediments are tell-tale indicators of depositional regimes. Based on the sedimentary structure, the Krol carbonates are characterized by eight facies associations: (1) deep subtidal; (2) shallow subtidal; (3) sand shoal; (4) peritidal carbonate complex; (5) lagoonal; (6) peritidal siliciclastic–carbonate; (7) incised valley fill; and (8) karstic fill. (Singh and Rai, 1978; Singh *et al.,* 1980; Jiang *et al.,* 2003a). When coupled with petrographic analyses, the post-depositional histories of these carbonate sediments belonging to different facies can be better understood. In the present work, some aspects of the sedimentological and petrographic features of Krol carbonates are discussed in the light of depositional setting and diagenetic evolution.

GEOLOGY AND STRATIGRAPHY

The Krol Belt (Auden, 1937) is confined to the central portion of the Lesser Himalaya. It comprises Himachal, Garhwal, and Kumaun regions (Fig. 1). The Krol belt extends over 350 km from Halog in the Shimla area to Nainital in

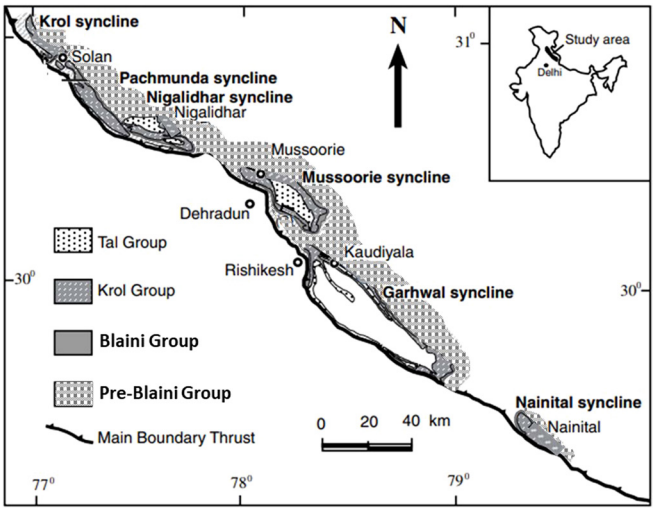

Fig. 1. Geological map of Krol Belt showing different synclines and lithogical units (modified after Jinag *et al*., 2003a).

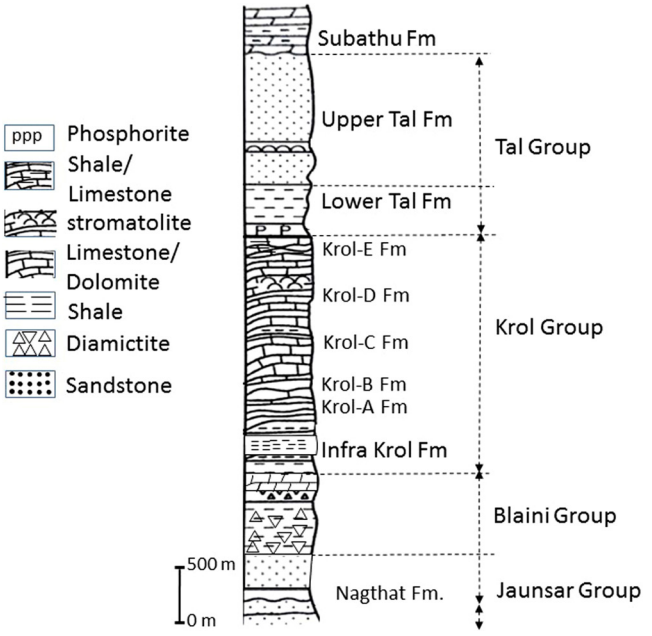

Fig. 2. Generalised lithostratigraphy of the Blaini, Krol and Tal Groups (modified after Mazumdar *et al*.,1999, Jain *et al*., 2020).

Kumaun. The southern limit of the Krol Belt is marked by folded Krol thrust, which coincides with the Main Boundary Fault in this region. Based on different foundation rocks and tectonic positions, Bhargava (1972, 79) classified the Krol belt into two parts, namely (i) outer Krol belt and (ii) inner Krol belt. The outer Krol belt has Shimla Group as its basement. It includes Pachmunda, Krol, Rajgarh, Khanog, and Sain Dhar synclines. The inner belt comprises Korgai, Nigalidhar, Mussoorie, Garhwal, and Nainital synclines. The broad stratigraphy of the inner Krol Belt is presented in figure 2. The Krol Group represents a thick succession of carbonate rocks with subordinate shale and sandstone (Fig. 2). The Krol Group is divided into Infra-Krol, Krol-A, Krol-B, Krol-C, Krol-D, and Krol-E Formations (Jain *et al.,* 2020). However, Shanker *et al.* (1993) and Shanker *et al.* (1997) recommended formal formation status as Mahi Formation (Krol A), Jarashi Formation (Krol B), and Kaudiyala Formations (Krol C, D, and E). The Tal Group (Fig. 2) overlies the Krol Group and is classified into Lower Tal Formation (Chert-black shale-phosphorite assemblages) and Upper Tal Formation (sandstone, quartz arenite).

METHODOLOGY

Leitz Orthoplan Stereomicroscope and M-8 Zoom Steriobinocular microscopes were used for the petrographic studies.

RESULTS AND DISCUSSION

Depositional Characteristics of Krol Group carbonates

The Krol-A is primarily a thinly laminated succession of micritic limestone and marl. It is well developed near Jharipani and Dhanaulti regions (Mussoorie syncline). The transition from Infra-krol to Krol-A is marked by an increase in carbonate content. Krol-A sequence primarily represents a deep subtidal depositional setting (Jiang *et al.,* 2003a).

The Krol-B is characterized by intercalated red and green shales. This unit is well developed throughout the Krol belt. Near Jharipani cm-thick recrystallized dolomite bands are present within the red shales. Isolated ripples and mud cracks (indicative of an intertidal environment) have been observed near Jharipani and Gulardogi. Near Dhanaulti, gray shales are interbedded with red and green shales. The transition from Krol-A to Krol-B is not associated with any major change in the depositional environment. Mineralogical studies show that detrital illite is the primary clay component with a subordinate amount of chlorite (Mazumdar, 1996). Detrital iron-oxide (fluvial supply) and iron-oxide coatings on other detrital components impart a reddish hue to the shales. In contrast to the siliciclastic detrital rich Krol-A and B lithologies, Krol-C and Krol-D are dominantly carbonate rocks and exhibit several distinct lithological characteristics. The lithofacies include cross-bedded oolitic carbonates, bedded massive micritic carbonate, algal and stromatolitic carbonate, well-developed tidal laminations, ripple laminations, and flaser beds (Mazumdar, 1996; Jiang *et al.,* 2002; 2003a).

The Krol-C is generally characterized by the presence of thick beds of dark gray, coarse-grained limestone, and dolomitic-limestone with interbedded thin to thick shale layers (0.5 to 2 m thick). Synsedimentary convoluted deformational structures (Fig. 3.1) are common within the carbonate beds. Early diagenetic chert lenses also show contorted features. Both erosional and solution-aided collapse breccia are seen within the dolomite beds. The breccia fragments are cemented by blocky calcite. Several

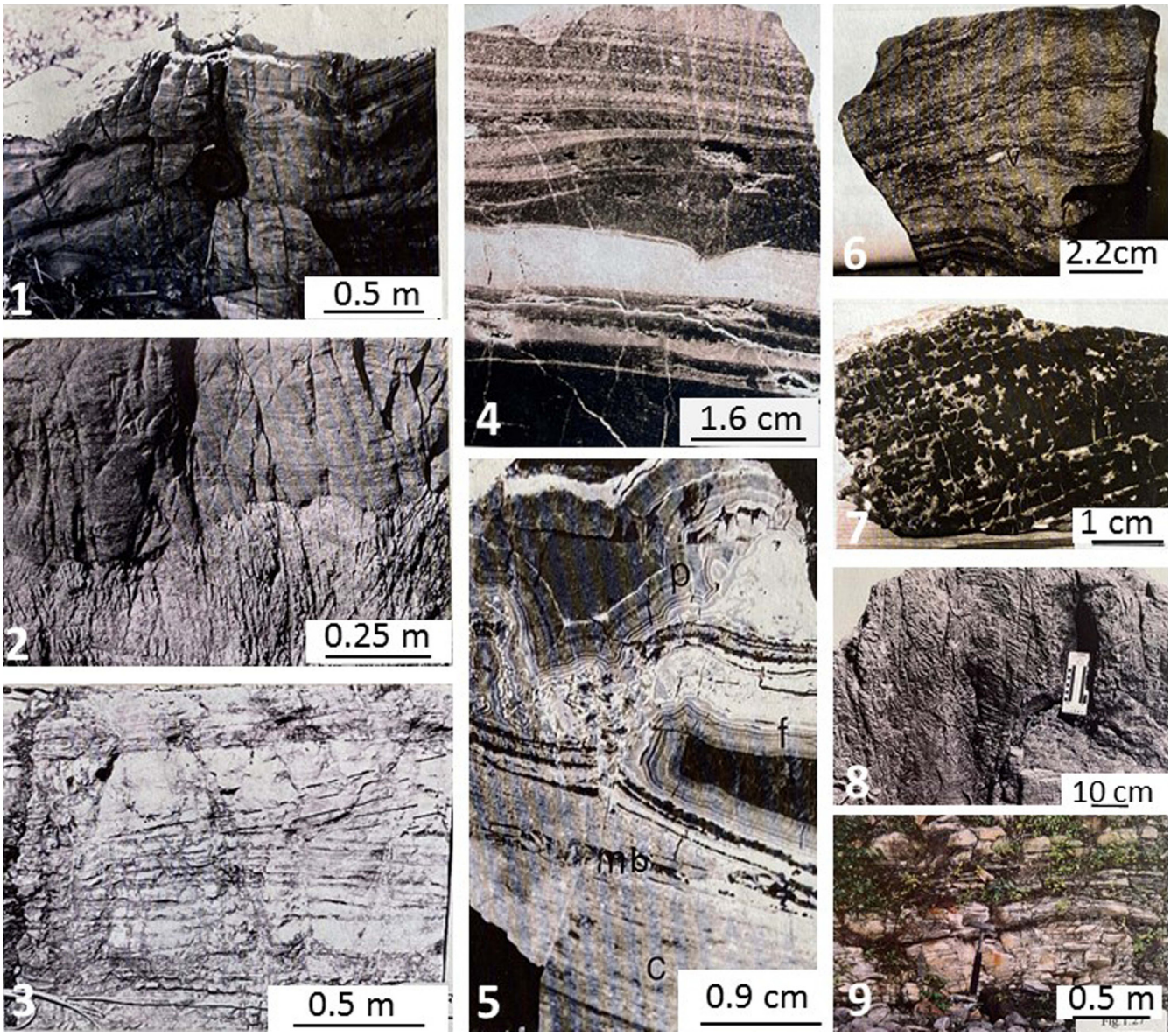

Fig. 3. Various depositional features recorded in the Krol carbonates. Fig. 3.1. Dolomite bed showing soft-sediment deformation structures; Fig. 3.2. Intrabasinal unconformity between dolomite beds. Note the difference in the color and nature of laminations; Fig. 3.3. Low angle cross-bedding in sandy dolomite beds; Fig. 3.4. Gray and white laminated dolomite of Krol-C with low angle cross-bedding; Fig. 3.5. Shallowing upward sequence in an algal mat facies of Krol-D showing cryptalgal laminites (C), pustular mats (P), fenestral vugs (F) and micro-brecciated (mb) zone; Fig. 3.6. Cryptalgal crinkled laminations and fenestral vugs (V); Fig. 3.7. Bluish gray Krol-C dolomite riddled with 'bird's eye' features. Fig. 3.8. Domal stromatolite near Suakholi; Fig. 3.9. Argillaceous carbonate of the Krol–E Formation.

unconformity surfaces (surfaces of emergence and erosion) were observed (Fig. 3.2) near Suakholi. These surfaces could be traced over a large area. Low angle cross-bedding (Fig. 3.3) and ripple marks are observed at some places. Gray and white laminated dolomites with low-angle cross-bedding (Fig 3.4) are exposed near Jharipani. Gypsum pockets present in Krol-C suggest supratidal evaporatic depositional conditions.

The Krol-D is well exposed near Barlowgunj iron bridge near Mussoorie and Gulardogi in the Garhwal Syncline. The dominantly dolomitic facies is characterized by the abundance of fenestrae, algal laminites, and pustular algal mats (Fig. 3.5). Argillaceous layers are almost absent in Krol-D. One of the most characteristic features of the peritidal carbonates of Krol-D is fine-scale laminations. These are on a millimeter-scale and are commonly associated with fenestral fabrics. Laminations are formed by the trapping of carbonate grains on the filamentous cyanobacterial mat (Fig. 3.6). Fenestral fabric (Flügel, 2010) is extensively developed in Krol-D carbonates. Both isolated bird's eye and laminoid fenestrae are common (Fig. 3.7). Dolomite intraclasts with microbial laminites and laminoid fenestrae (Tucker, 1983) are present within the fenestral facies and often display cyclic patterns. These features indicate an upper intertidal to supratidal environment of deposition. Both columnar and domal interconnected stromatolites (Fig.3.8) have been recorded from Krol-D dolomite (Misra, 1984; Tewari and Qureshy, 1985; Mazumdar, 1996; Jiang *et al.,* 2003a). The transition from the Krol-D to Krol-E shows a gradual

increase in argillaceous input accompanied by a decrease in the dominance of carbonate sedimentation (Fig. 3.9).

The Krol-E is well exposed in various sections of the Mussoorie Syncline and near Kaudiyala village in the Garhwal Syncline. A gradual transition from compact dolomite to argillaceous dolomite not only indicates a change in depositional but also points towards a climatic change from arid to semiarid-humid conditions. Pyrite is ubiquitously present as disseminated grains in the argillaceous dolomite. Krol-E sediments represent a subtidal depositional setting (Jiang *et al.,* 2003a).

Petrographic characteristics of Krol carbonates and genesis

Fenestral void filling (fibrous dolomite)—.The fenestral void filling type (Fig. 4.1 and 4.2) resembles the type 'A' dolomite of Tucker (1983). The fibrous dolomites form an isopachous layer within the fenestral cavities. The width of the crystals increases towards the center of the cavity. The carbonate grains show orientation perpendicular to the cavity walls. Most crystals are clouded due to fluid or mineral inclusions and show unit extinction. Such a texture is designated as 'radial fibrous' (Richter *et al.,* 2011, 2015; Zhao *et al.,* 2021). Two isopachous fibrous layers come into contact (during growth) along a plane at the corners of the cavities. The compromise boundary remains straight as long as the growth rate and the angle between the crystal faces remain the same. The substrate-parallel laminae show distinct variations in color. The alternation of light and dark brown shades is due to variation in the content of organic matter, Fe-oxide or mineral inclusions. It often gives rise to pseudopleochroism. The fibrous crystals grow by accretion parallel to the substrate. Tucker (1982) explained that such fibrous dolomites are of primary origin, i.e., direct precipitation of dolomite from hypersaline water with a very high Mg/Ca ratio. However, they may be synsedimentary or early diagenetic dolomitization (mimically replaced) of an acicular precursor. Excellent preservation of the original textural details and the absence of any discordant dolomite phase further support the early diagenetic origin of the texture (Zempolich *et al.,* 1988).

Fascicular optic type (Kendall, 1985; Zhao *et al*., 2021) fibrous texture (Fig. 4.3 and 4.4) resembles type 'C' dolomite of Tucker (1983). The wedge-shaped crystals (Fig. 4.3) show the radial arrangement of the curved sub-crystals. Individual crystals show diverging undulatory extinction (Fig. 4.4) due to different optical orientations of the sub-crystals which fan out from a point on the substrate. The crystal boundaries are non-planar and often quite irregular due to neomorphic adjustments and competitive growth fabric. Individual crystals are broadly wedge-shaped. The wedges originated from the coalescence of crystallites from the original cement during the neomorphic process. Crystallographic coalescence of splays produces the wedge-shaped fascicular optic dolomite.

Dedolomitisation Texture—.Well preserved dedolomitisation texture has been observed in the Krol dolomites near Buranskhand (Mazumdar, 1996). Polycrystalline euhedral rhombs of calcite (Fig. 4.5) are scattered within a microsparite groundmass. The grain margins are rather blurred due to recrystallization. The microspars of the groundmass are more turbid than the clearer drusy crystals filling the rhombs. Both earlier and more recent studies (De Groot, 1967; Evamy, 1967; Chillinger *et al.,*1979; Vandeginste and John, 2012; Makhloufi and Samankassou, 2019) have attributed dedolomitization primarily to surface weathering processes including karst formation (Kupecj and Land, 1991) involving meteoric water-dolomite and evaporite interaction. Dissolution of evaporites ($CaSO_4$) by meteoric water circulation is apparently responsible for excess Ca^{2+} ions driving dedolomitization. Widely observed enrichment of Fe^{3+} (hematite) in dedolomitized zones is attributed to the oxidation of Fe^{2+} during weathering processes (Braun and Friedman, 1969; Vandeginste and John, 2012). However, in contrast to weathering hypothesis and karstification, Schoenherr *et al.* (2018) proposed a pressure solution pathway (due to burial) responsible for the conversion of gypsum to anhydrite which enhances Ca^{2+} ion concentrations in the percolating groundwater facilitating dedolomitization.

Cloudy Center Clear Rim Dolomite (CCCR texture)—. Dolomites with CCCR texture (Fig. 4.6) are characterized by a mosaic of coarse (80 in 100 μm), interlocking, anhedral to subhedral crystals with mostly sutured or irregular grain boundaries. Fe-oxide is concentrated at several crystal boundaries with small and sharp embayments depicting dissolution at grain boundaries. The distribution of cloudiness (remnant of precursor calcite and/or inclusions) is both patchy (transgressing the crystal boundaries) and intracrystalline. The latter has been described as 'cloudy center clear rim dolomite' (CCCR). The cloudy patches probably represent the remnant of low Mg calcite (LMC) (Sibley, 1982; Sibley and Gregg,1987). The grains are riddled with Fe-oxide granules and flaky minerals. The CCCR type possibly represents moderate to deep burial dolomitization (Zhang *et al.,* 2017).

Baroque Dolomite—.Several dolomite samples from the Suakholi region display features resembling baroque or saddle dolomite (Radke and Mathis, 1980). Saddle dolomites are characterized by curved cleavage planes, curved crystal faces, and sweeping extinction (Fig. 5.1). The crystals are ~1mm or more in size and highly clouded due to the presence of calcite relicts, fluid inclusions, or Fe-oxide granules. The overall texture can be described as a xenotropic mosaic of coarse dolospars with non-planar crystal boundaries and crystal faces and cleavage planes. Such dolomites occur in small pockets. According to Radke and Mathis (1980), pronounced variations in the composition of individual crystals are common giving rise to distinct zonations. The lattice distortion observed in the baroque dolomite is due to variations in the concentration of the Ca^{2+} ions adsorbed onto the growing crystal surfaces. Based on backscattered SEM, Searl (1989) attributed lattice distortion in saddle dolomites to the incorporation of extra lattice layers at propagating crystal edges, relative to face centers. Saddle dolomites are reported as cavity filling crystals in hydrocarbon reservoirs, paleoaquifers, and the Pb-Zn mineralization zone in the form of gangue minerals (Spotl and Peatman, 1998; Benles and Hardy, 1980). Based on petrography and stable isotopic studies by Srinivasan (1994), and Zenger (1983) have shown that saddle dolomites are of burial diagenetic origin (Tucker and Wright, 1990).

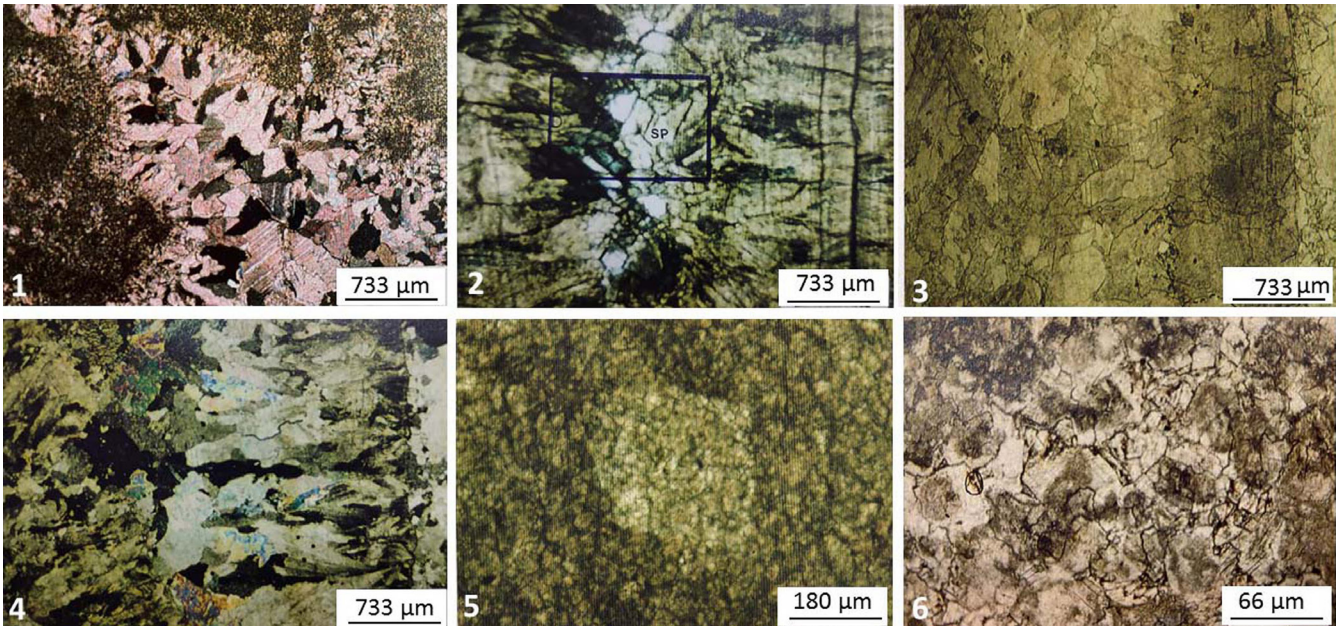

Fig. 4. Petrographic characteristics of the Krol carbonates. Fig. 4.1. Fenestral void filling texture showing inward growth of dolomite crystals. A narrow zone of dolomite crystals within accretionary laminae is followed by coarse dolospars with well-developed twin laminae and straight grain contacts. Cross polarised; Fig. 4.2. Dolomite with 'radial fibrous' texture showing accretionary growth layers, fibrous dolomite. The black square shows the co-occurrence of radial fibrous and sparry crystals (D) and late-stage dolospars (SP). Plane polarised; Fig. 4.3. Same as above under plane polarised light showing grain boundaries of wedge-shaped crystal delineated in the figure; Fig. 4.4. Dolomite with 'fascicular radial optic' texture showing the arrangement of curved sub-crystals and diverging extinctions. Note sutured contacts between the acicular cystals due to growth pressure. Cross polarised; Fig. 4.5. Dedolomitisation texture showing polycrystalline euhedral rhombs of calcite in a microsparitic groundmass. Plane polarised; Fig. 4.6. Cloudy center clear rimmed dolomite (CCCR) texture showing patchy remnant (cloudy) of calcite within euhedral to subhedral dolomite with planar to sutured contacts. Plane polarised.

Chert-Dolomite Association—.Microcrystalline chert is common in Krol carbonates. It is present in the form of thin layers, nodules, deformed lenses (soft-sediment deformation structure), and chert breccia (Fig. 5.2) cemented by dolospar. Chert fragments show large variability in size with the patchy development of fibrous silica. Fragmentation of the chert layers possibly results from the cracking of semi-consolidated silica gel during subaerial exposures. The replacement origin of the chert is well displayed by the presence of irregular/embayed contacts (Fig. 5.3) with dolomite and the presence of relic dolorhombs with corroded margins within cherts. The deep brown color of the embayed margin of the dolomite compared to relict rhombs indicate the leaching and enrichment of iron during the replacement of carbonate by silica in oxidizing and alkaline conditions. In the absence of SiO_2-precipitating organisms (radiolarians, sponges, and diatoms) in the Late Neoproterozoic, the chert layers may be attributed to direct precipitation from seawater at the sediment-water interface (Maliva *et al.,* 1989; Siever, 1991; Al Rajaibi *et al.,* 2015; Conley *et al.,* 2017). Association of chert with peritidal limestone/dolomite is widely reported from Neo and Mesoproterozoic peritidal carbonates (Horodyski and Donaldson, 1983; Lowe, 1983; Knoll, 1985; Maliva *et al.,* 1989 and 2005). Growth of fibrous silica in the pressure shadows (Fig. 5.4) surrounding pyrite has been observed in dolomites containing abundant detrital quartz. This may be attributed to the dissolution and reprecipitation of silica (within pressure shadows) during burial diagenesis.

Oolites—.Both mud-supported (Fig. 5.5) and grain-supported (Fig. 5.6) oolitic limestone and dolomites are recorded from the Krol carbonates (Krol-C and D). The grain-supported oolitic texture shows post compactional recrystallization. Each oolite grain consists of an isopachous rim of microspar and a central coarse dolospar (Fig. 6.1) with well-developed twin lamellae. The rim is clouded compared to the central clear dolospar. No nucleus could be detected.

Structure Grumeleuse—.Figure-6.2 resembles 'structure grumeleuse' or clotted limestone type texture. Bathurst (1972) reviewed this texture and discussed the diagenetic significance. It appears as isolated or merged clots of extremely finely crystalline calcite standing out as patches in a matrix of granular calcite (McKenzie *et al.,*1980; Webb, 1987; Batten *et al.,* 2004). The clots are globular or irregular in shape and lack internal differentiation of any kind. It is a two-component fabric, consisting of patches of micrite embedded in a matrix of microspars. Alizarin stained thin sections show that the groundmass is composed of dolo-microspar and the globular patches (dark under crossed nicols) are of calcite. Within the microsparitic groundmass there are irregular patches of coarse dolospar representing aggradational neomorphic grain growth.

Cementation of Algal Mat Fragments—.The micritic algal mat fragments are cemented by thin isopachous layers of fibrous crystals and coarse, anhedral, equant dolospars with straight contacts (Fig. 6.3). The original fabric is well preserved. The algal mat fragments are disrupted along desiccation cracks as a result of subaerial exposures in a supratidal environment. The intraclast voids were subsequently filled by early diagenetic cement The neomorphic growth of the crystals during early meteoric diagenesis further displaced the mat fragments

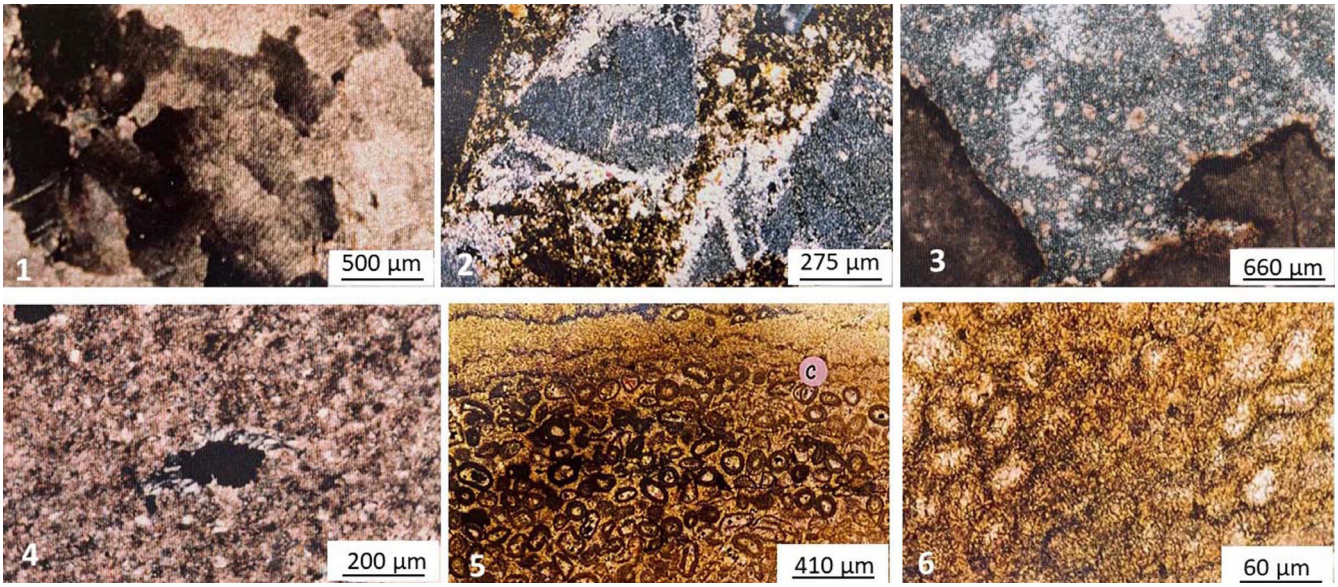

Fig. 5. Petrographic Characteristics of the Krol carbonates. Fig. 5.1. Baroque (or saddle) dolomite showing curved cleavage planes and undulose extinction. Cross polarised; Fig. 5.2. Partially recrystallised chert fragments cemented by ferrugenous dolospars. Cross polarised; Fig. 5.3. Irregular embayed contact between chert and dolomite. Note the presence of relict dolorhombs within chert. Locally fibrous habit is developed. Cross polarised; Fig. 5.4. Development of fibrous quartz within pressure shadow around a pryrite cluster. Cross polarised; Fig. 5.5. Mud supported oolitic fabric with few grain contacts. Some grains are broken due to compaction (c). Cross polarised; Fig. 5.6. Magnified view of the recrystallised oolites showing grain volume loss due to compaction and suturing.

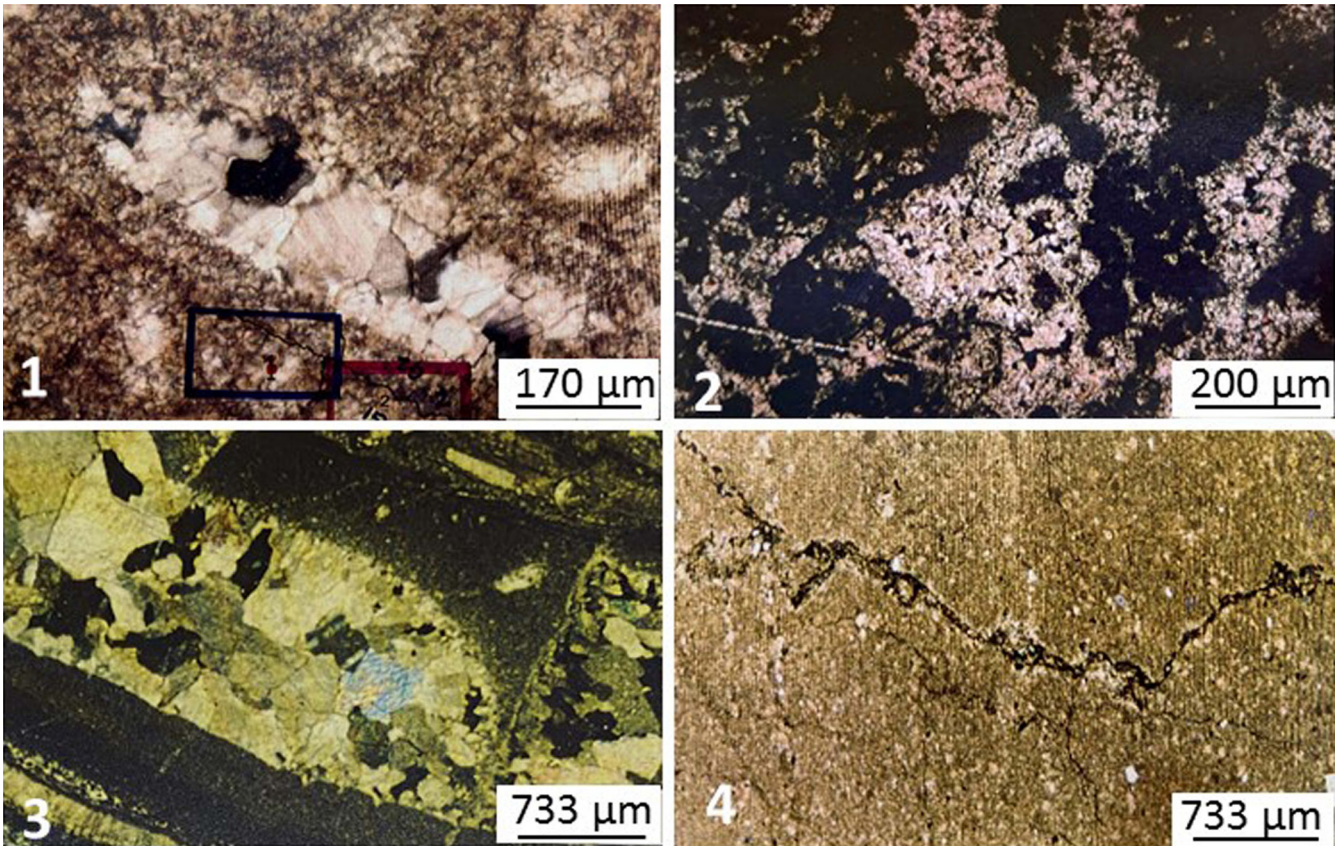

Fig. 6. Petrographic Characteristics of the Krol carbonates. Fig. 6.1. Recrystallised oolites showing evidence of compaction and deformation. The black square demarcates the sutured compaction zone. Recrystallisation resulted in blurring of grain contacts. Plane polarised; Fig. 6.2. Isolated and merged clots of fine grained calcite within dolomicrosphoritic groundmass (structure grumeluse type texture). Cross polarised; Fig. 6.3. Algal mat fragments cemented by dolospars (syndepositional cementation). Cross polarised; Fig. 6.4. Non-sutured anastomosing microstylolite in detrital rich dolomite. Cross polarised.

(displacive texture). The early cementation prevented burial compaction.

Anastomosing microstylolitic (non-sutured) seam solution—.This type of pressure solution feature (Fig. 6.4) is abundant in the detrital-rich dolomicrosparites of Krol-E. Stylolitisation is the result of post-dolomitization burial diagenesis. Microstylolites are very thin undulatory surfaces with relief to the order of 20 to 40 microns. Limestones/ dolomites that have a significant amount of clayey or silty materials (IR) tend not to have sutured seams (Mujtaba *et al.,* 2004). Pressure solution features in carbonate rocks form due to preferential dissolution of minerals at points of stress. Crystal deformation at the stressed contacts enhances solubility. The distribution of strain at the surfaces of grains near their points of contact is a function of grain orientation, size and shape, and anisotropy of the crystal lattice and crystal mosaic.

CONCLUSIONS

Petrographic studies of the Krol Carbonates reveal various early and burial diagenetic textures. The observations show that the dolomitization of the Krol carbonates was primarily an early diagenetic process. The early diagenetic textures are well preserved in all the carbonate units of the Krol Group, although evidence of burial diagenesis has also been recorded. It is interesting to note that dolomitization has not destroyed the early diagenetic textures. Well preserved radial fibrous and fascicular optic type dolomite have been recorded from the Krol-C and Krol-D carbonates, reflecting early cementation phases. Columnar dolomite crystals are common and well preserved as cement in the intraclasts. Similar textures have been recorded in the fenestral vugs where two stages of (early and late stage) dolomite cement have been documented through SEM photographs. Such fibrous dolomites appear to be primary in origin, i.e., direct precipitation of dolomite from hypersaline water with a very high Mg/Ca ratio (Tucker, 1982). However, direct precipitation of structurally stable and stoichiometrically perfect dolomite has so far not been recorded from carbonate rocks. Much of the fibrous dolomites of the Krol Group are probably of replacement origin (mimically replaced) i.e., synsedimentary or early diagenetic dolomitization of an acicular precursor. Excellent preservation of the original textural details and the absence of any discordant dolomite phase further support the early diagenetic dolomitization. Apart from early diagenetic columnar dolomites, early-stage dolospars have also been recorded as blocky cement within algal mat fragments. The existence of heterogeneity in the texture and structure at both micro and mesoscopic scale indicate that dolomitization did not result in obliteration and homogenization of the early stage textural features. Burial diagenetic features are represented by baroque dolomites, stylolites (sutured and non-sutured), coarse crystals with sutured grain contacts, recrystallized oolites showing grain volume loss and growth of fibrous quartz crystals in pressure shadow around the rigid pyrite grains.

ACKNOWLEDGEMENTS

Financial support for this work was received from CSIR. Discussion with Prof. I.B. Singh greatly benefitted in understanding the carbonate peritidal system. This article is based on the Ph.D. thesis awarded by the University of Delhi in 1996. I am thankful to Prof. D. M. Banerjee for inviting me to contribute this article for Prof. I.B. Singh Memorial Volume.

REFERENCES

Aharon, P., Schidlowski, M. and Singh, I. B. 1987. Chronostratigraphic markers in the end-Precambrian carbon isotope record of the Lesser Himalaya. Nature, 327*:* 699-702.

Al Rajaibi, I. M., Hollis, C. and Macquaker, J. H. 2015. Origin and variability of a terminal Proterozoic primary silica precipitate, Athel Silicilyte, South Oman salt basin, Sultanate of Oman. Sedimentology, 62(3): 793-825.

Auden, J. B. 1937. Structure of the Himalaya in Garhwal. Records Geological Survey of India,71: 407-433.

Bathurst, R. G. C. 1972. Carbonate sediments and their diagenesis. p. 1-658. In: Developments in Sedimentology (Ed: Bathurst, R.G. C) Elsevier (Amsterdam). 657p.

Batten, K. L., Narbonne, G. M. and James, N. P. 2004. Paleoenvironments and growth of early Neoproterozoic calcimicrobial reefs: platformal Little Dal Group, northwestern Canada. Precambrian Research, 133(3-4): 249-269.

Becker, S., Reuning, L., Amthor, J. E. and Kukla, P. A. 2019. Diagenetic processes and reservoir heterogeneity in salt-encased microbial carbonate reservoirs (Late Neoproterozoic, Oman). Geofluids, 2019: 1-19.

Benles, F. W. and Hardy, J. W.1980. Criteria for the recognition of diverse dolomite types with an emphasis on studies on host rocks for Mississippi valley type ore deposit, p.197-213. In: Concepts and Models of Dolomitization (Eds. Zenger, D. H., Dunham, J. B. and Ethington, R. L.), SEPM Special Publication.

Bhargava, O. N. 1972. Reinterpretation of the Krol belt. Himalayan Geology, 2: 47-81.

Bhargava, O. N. 1979. Lithostratigraphic Classification of the Blaini, Infra Krol, Krol and Tal Formations-A Review. Journal of the Geological Society of India 20: 7-16.

Chilingar, G. V., Zenger, D. H., Bissell, H. J. and Wolf, K. H. 1979. Dolomites and dolomitization, p., 423–536, In: Diagenesis in Sediments and Sedimentary Rocks (Eds. Larsen, G. and Chillingar, G. V), Developments in sedimentology, Elsevier (Amsterdam).

Conley, D. J., Frings, P. J., Fontorbe, G., Clymans, W., Stadmark, J., Hendry, K.R., Marron, A.O. and De La Rocha, C.L. 2017. Biosilicification drives a decline of dissolved Si in the oceans through geologic time. Frontiers in Marine Science, 4: 397.

DeGroot, K. 1967. Experimental dedolomitization. Journal of Sedimentary Research, 37(4): 1216-1220.

Evamy, B.D. 1967. Dedolomitization and the development of rhombohedral pores in limestones. Journal of Sedimentary Research, 37(4): 1204-1215.

Flügel, E. 2010.Microfacies of carbonate rocks: analysis, interpretation and application. 984p, Springer Berlin (Heidelberg).

Horodyski, R. J. and Donaldson, J. A. 1983. Distribution and significance of microfossils in cherts of the middle Proterozoic Dismal Lakes Group, District of Mackenzie, Northwest Territories, Canada. Journal of Paleontology, 57(2): 271-288.

Hussain, S. A., Han, F. Q., Ma, Z., Hussain, A., Mughal, M. S., Han, J., Alhassan, A., and Widory, D. 2021. Unraveling sources and climate conditions prevailing during the deposition of Neoproterozoic evaporites using coupled chemistry and boron isotope compositions (δ11B): the example of the salt range, Punjab, Pakistan. Minerals, 11(2): 1-15.

Jain, A.K., Banerjee, D.M., and Kale, V.S., 2020, Tectonics of the Indian Subcontinent: Cham, Switzerland, Springer Nature, 576p.

Jiang, G., Christie-Blick, N., Kaufman, A. J., Banerjee, D. M. and Rai, V. 2002. Sequence stratigraphy of the Neoproterozoic infra Krol formation and Krol Group, lesser Himalaya, India. Journal of Sedimentary Research, 72(4): 524-542.

Jiang, G., Christie-Blick, N., Kaufman, A. J., Banerjee, D. M. and Rai, V. 2003a. Carbonate platform growth and cyclicity at a terminal Proterozoic passive margin, Infra Krol Formation and Krol Group, Lesser Himalaya, India. Sedimentology, 50(5): 921-952.

Jiang, G., Kennedy, M. J. and Christie-Blick, N. 2003b. Stable isotopic evidence for methane seeps in Neoproterozoic postglacial cap carbonates. Nature, 426: 822-826.

Jiang, G., Kennedy, M.J., Christie-Blick, N., Wu, H. and Zhang, S. 2006. Stratigraphy, sedimentary structures, and textures of the late Neoproterozoic Doushantuo cap carbonate in South China. Journal of Sedimentary Research, 76(7): 978-995.

Jiang, G., Sohl, L. E., & Christie-Blick, N. 2003c. Neoproterozoic stratigraphic comparison of the Lesser Himalaya (India) and Yangtze block (south China): Paleogeographic implications. Geology, 31(10): 917-920.

Kaufman, A. J., Jiang, G., Christie-Blick, N., Banerjee, D. M. and Rai, V. 2006. Stable isotope record of the terminal Neoproterozoic Krol platform in the Lesser Himalayas of northern India. Precambrian Research, 147(1-2): 156-185.

Kendall, A. C. 1985 Radiaxial fibrous calcite: a reappraisal. 36: 59-77, In: Carbonate Cements. (Eds. Schneidermann, N and Harris, P. M.), Special Publication, Society Economic Palaeontology.

Knoll, A. H. 1985. Exceptional preservation of photosynthetic organisms in silicified carbonates and silicified peats. Philosophical Transactions of the Royal Society of London. B, Biological Sciences, 311: 111-122.

Kupecz, J. A. and Land, L. S. 1991. Late-stage dolomitization of the lower Ordovician Ellenburger group, west Texas. Journal of Sedimentary Research, 61(4):551-574.

Lowe, D. R. 1983. Restricted shallow-water sedimentation of Early Archean stromatolitic and evaporitic strata of the Strelley Pool Chert, Pilbara Block, Western Australia. Precambrian Research, 19(3): 239-283.

Makhloufi, Y. and Samankassou, E. 2019. Geochemical constraints on dolomitization pathways of the Upper Jurassic carbonate rocks in the Geneva Basin (Switzerland and France). Swiss Journal of Geosciences, 112(2): 579-596

Maliva, R. G., Knoll, A. H. and Siever, R. 1989. Secular change in chert distribution: a reflection of evolving biological participation in the silica cycle. Palaios, 4: 519-532.

Maliva, R. G., Knoll, A. H. and Simonson, B. M. 2005. Secular change in the Precambrian silica cycle: insights from chert petrology. Geological Society of America Bulletin, 117(7-8): 835-845.

Mazumdar, A. 1996. Petrographic and geochemical characterization of the Neoproterozoic-Cambrian succession in a part of the Krol Belt, Lesser Himalaya. Ph. D. Thesis, University of Delhi.

Mazumdar, A. and Banerjee, D. M. 1998. Siliceous sponge spicules in the Early Cambrian chert-phosphorite member of the Lower Tal Formation, Krol belt, Lesser Himalaya. Geology, 26(10): 899-902.

Mazumdar, A., Banerjee, D.M., Schidslowski, M., and Balram, V. 1999. Rare-earth elements and stable isotopic geochemistry Early Cambrian, Lower Tal chert-phosphorite of Krol Belt, Lesser Himalaya, India. Chemical Geology, 156: 275-297.

Mazumdar, A. and Strauss, H. 2006. Sulfur and strontium isotopic compositions of carbonate and evaporite rocks from the late Neoproterozoic–early Cambrian Bilara Group (Nagaur-Ganganagar Basin, India): Constraints on intrabasinal correlation and global sulfur cycle. Precambrian Research, 149(3-4):217-230.

McKenzie, J. A. and Kelts, K. R. 1980. A study of interpillow limestones from the M-Zero anomaly, Leg 51, Hole 417D, p. 753-769. In: Initial Reports of the Deep Sea Drilling Project (Ed. Donnelly, T., *et al.,*), Texas A & M University College of Geosciences.

Misra, S. B. 1984. Depositional environment of the Krol Group of the Nainital area and its impact on the stromatolites. Proceedings of the Indian Academy of Sciences-Earth and Planetary Sciences, 93(4): 447-464.

Mujtaba, M., Noor, I. and Ali, S. 2004. Depositional Environment, Diagenetic Alteration and Porosity Development in the Early Eocene Carbonates, Encountered in Adhi-7 Well, Potwar, Pakistan. Pakistan Journal of Hydrocarbon Research, 14: 19-33.

Radke, B. M. and Mathis, R. L. 1980. On the formation and occurrence of saddle dolomite. Journal of Sedimentary Petrology, 50(4): 1149-1168.

Richter, D. K., Immenhauser, A., Neuser, R. D. and Mangini, A. 2015. Radiaxial-fibrous and fascicular-optic Mg-calcitic cave cement: a characterization using electron backscattered diffraction (EBSD). International Journal of Speleology, 44(1): 91-98

Richter, D. K., Neuser, R. D., Schreuer, J., Gies, H. and Immenhauser, A. 2011. Radiaxial-fibrous calcites: A new look at an old problem. Sedimentary Geology, 239(1-2): 23-36.

Schmid, S. 2017. Neoproterozoic evaporites and their role in carbon isotope chemostratigraphy (Amadeus Basin, Australia). Precambrian Research, 290: 16-31.

Schoenherr, J., Reuning, L., Hallenberger, M., Lüders, V., Lemmens, L., Biehl, B.C., Lewin, A., Leupold, M., Wimmers, K. and Strohmenger, C.J., 2018. Dedolomitization: review and case study of uncommon mesogenetic formation conditions. Earth-science reviews,185: 780-805

Searl, A. 1989. Saddle dolomite: a new view of its nature and origin. Mineralogical Magazine, 53(373): 547-555.

Shanker, R., Kumar, G, Mathur, V. K and Joshi, A. 1993. Stratigraphy of the Blaini, InfraKrol, Krol and Tal succession, Krol Belt Lesser Himalaya. Indian Journal of Petroleum Geology, 2(2): 99-136.

Shanker, R., Mathur, V. K., Kumar, G. and Srivastava, M. C. 1997. Additional Ediacaran biota from the Krol Group, Lesser Himalaya, India and their significance. Geoscience Journal, 18:79-94.

Sibley, D. F. 1982. The origin of common dolomite fabrics. Journal of Sedimentary Petrology, 52: 987-998.

Sibley, D. F. and Gregg, J. M. 1987. Classification of dolomite rock textures. Journal of Sedimentaryy Research, 57(6): 967-975.

Siever, R., Schneider, S. H. and Boston, P. J. 1991. Silica in the oceans: biological-geochemical interplay. p. 287–295. In: Scientists on Gaia (Eds. Schneider, S. H. and Boston, P. J.), Cambridge, MA: MIT Press.

Singh, I. B., Bhargava, A. K. and Rai, V. 1980. Some observations on the sedimentology of the Krol Succession of Mussoorie Area, Uttar Pradesh. Journal of Geological Society of India, 21(5): 232-238..

Singh, I. B. and Rai, V. 1978. Some observations on the depositional environments of the Krol Formation in the Nainital area. Himalayan Geology, 8(2): 633-656.

Singh, I. B. and Rai, V. 1983. Fauna and biogenic structures in Krol-Tal succession (Vendian-Early Cambrian), Lesser Himalaya: their biostratigraphic and palaeoecological significance. Journal of the Palaeontological Society of India, 28:67-90.

Spötl, C. and Pitman, J. K. 1998. Saddle (baroque) dolomite in carbonates and sandstones: a reappraisal of a burial-diagenetic concept, p.437-460. In: (Ed. Morad, S), Wiley (New Jersey).

Srinivasan, K., Walker, K. R. and Goldberg, S. A. 1994. Determining fluid source and possible pathways during burial dolomitization of Maryville Limestone (Cambrian), Southern Appalachians, USA. Sedimentology, 41(2):293-308.

Tewari, V.C., and Qureshy, M. F. 1985. Algal structures from the Upper Krol-Lower Tal formations of Garhwal and Mussoorie synclines and their palaeo-environmental significance. Journal of Geological Society of India, 26: 111-117

Tucker, M. E. 1982. Precambrian dolomites: petrographic and isotopic evidence that they differ from Phanerozoic dolomites. Geology, 10(1): 7-12.

Tucker, M. E. 1983. Diagenesis, geochemistry, and origin of a Precambrian dolomite; the Beck Spring Dolomite of eastern California. Journal of Sedimentary Research, 53(4): 1097-1119.

Tucker, M. E and Paul Wright, V. 1990. Carbonate Sedimentology Blacwell Scientific Publication (New Jersey).482p.

Vandeginste, V. and John, C. M. 2012. Influence of climate and dolomite composition on dedolomitization: insights from a multi-proxy study in the central Oman Mountains. Journal of Sedimentary Research, 82(3): 177-195.

Webb, G. E. 1987. Late Mississippian thrombolite bioherms from the Pitkin Formation of northern Arkansas. Geological Society of America Bulletin, 99(5): 686-698.

Xiao, S., Jiang, G., Ye, Q., Ouyang, Q., Banerjee, D. M., Singh, B. P., Muscente, A. D., Zhou, C and Hughes, N. C. 2022. Systematic paleontology, acritarch biostratigraphy, and $\delta^{13}C$ chemostratigraphy of the early Ediacaran Krol A Formation, Lesser Himalaya, northern India. Journal of Paleontology, 1-62, doi:101017/jpa.2022.7.

Xiao, S., Shen, B., Tang, Q., Kaufman, A.J., Yuan, X., Li, J. and Qian, M. 2014. Biostratigraphic and chemostratigraphic constraints on the age of early Neoproterozoic carbonate successions in North China. Precambrian Research, 246: 208-225.

Zempolich, W. G., Wilkinson, B. H. and Lohmann, K. C. 1988. Diagenesis of late Proterozoic carbonates; the Beck Spring Dolomite of eastern California. Journal of Sedimentary Research, 58(4): 656-672.

Zenger, D. H. 1983. Burial dolomitization in the Lost Burro Formation (Devonian), east-central California, and the significance of late diagenetic dolomitization. Geology, 11(9): 519-522.

Zhang, L., Jiao, Y., Rong, H., Li, R. and Wang, R. 2017. Origins and geochemistry of oolitic dolomite of the feixianguan formation from the yudongzi outcrop, Northwest Sichuan Basin, China. Minerals, 7: 2-21.

Zhao, D., Tan, X., Hu, G., Wang, L., Wang, X., Qiao, Z., Luo, S. and Tang, H. 2021. Characteristics and primary mineralogy of fibrous marine dolomite cements in the end-Ediacaran Dengying Formation, South China: Implications for aragonite–dolomite seas. Palaeogeography, Palaeoclimatology, Palaeoecology, 581: 1-13.